ON THE VELOCITY FIELD OF A FREE OVERFALL

Chang Lin, Wen-Yen Huang, Horng-Fure Suen, and Guang-Heui Yen
Department of Civil Engineering, National Chung Hsing University,
Taichung, Taiwan 402, R.O.C.

ABSTRACT

The characteristics of the velocity field of a free overfall (including the velocity profiles of and near the sliding jet, and in the pool) are investigated experimentally, using a novel flow visualization technique as well as fiber laser Doppler velocimetry (FLDV). The range of Froude number for the approaching flow upstream of a drop structure is from 0.75 to 1.32. Several detailed flow structures, regarding the mean horizontal velocity distributions and the circulating vortex flow inside the pool of a drop structure, are elucidated in the present study. An unique similarity profile of the mean horizontal velocity measured inside the pool is proposed both for supercritical and subcritical approaching flow conditions.

INTRODUCTION

The phenomenon of the "free overfall or vertical drop" meaning the stream flow in the neighborhood of a sharp drop structure — can be seen frequently in both natural and artificial channels. For example, the flow running over a weir constructed across a river is the most common one. Free overfalls are also formed by river bed erosion at the downstream side of bed protection works which are built to control the slope or elevation of river bed.

A comprehensive knowledge of the flow characteristics through the drop structure is useful in the design of a suitable stilling basin required for energy dissipation in such a structure . In the past, the external flow fields, such as the upper and lower free surface profiles of the nappe, the length and depth of the pool, and the energy loss of a free overfall, were studied extensively.

To the best of the authors' knowledge, fundamental in this field was the study carried out by Rouse (1936). An experimental investigation of the hydraulics of free overfalls, with the subcritical flow approaching the drop structure, was made by Moore(1943). He indicated that the energy loss at the drop could be significant depending on the relative height of the drop. White (1943) developed a theoretical solution to predict the energy loss based upon several assumptions, which have been questioned and modified by Gill (1979) and Rajaratnam and Chamani (1995). Rand (1955) proposed some empirical equations to describe the characteristics of free overfalls using a dimensionless parameter, known as Drop number. Recently, Marchi (1993) presented an analytic model to predict the nappe lower profile and upstream water-surface profile applicable to upstream subcritical and supercricital flow conditions. The velocity profiles of the falling jet as well as of and near the sliding jet of a free overfall were first investigated by Rajaratnam and Chamani (1995), using two different Prandtl probes with external diameters of 2.6 and 3.2 mm. However, many detailed flow structures concerning velocity field, circulating vortex flow, wall shear stress, and mechanism of energy loss inside the pool of a free overfall are not fully understood until now.

The purpose of the present study is to make clear the characteristics of velocity field in the sliding jets and inside the pools of two-dimensional free overfalls, employing flow visualization technique and fiber laser Doppler velocimetry (FLDV).

EXPERIMENTAL SETUP AND TECHNIQUES

The experiments were conducted in a free surface water channel with a 305.0 cm long working section, 50.0 cm wide by 54.0 cm deep. The working section was enclosed by glass windows on both sides and bottom to allow visual and optical study of the flow throughout its full length. Three layers of perforated steel plate (which were installed in the upstream settling plenum), one piece of honeycomb 10.0 cm in length, four meshes with different grid sizes, and a specially designed 3-D contraction were used to remove any large-scale irregularities and to smooth the inlet flow. In order to achieve quite stable flow in this water channel, the pumping system was monitored by a speed-control unit with a shaft feedback circuit.Two fully ventilated drop structures of heights of 11.0 and 20.0 cm were installed in the working section. The free surface profiles upstream of a drop, along the falling and sliding jets, and of the pool were all measured by a precision point gauge. Experiments for flow visualization study were carried out using the aluminum particle tracking technique. The light source was a 7 W argon-ion laser tube (Coherent Innova 90-4), from which a laser beam was emitted and spread into a fan-shaped light sheet (about 1.3 mm thick) by a cylindrical lens. The laser tube was installed just beneath the bottom glass of the working section. The light sheet was used to illuminate the two-dimensional motion of particle traces in the sliding jet and inside the pool of a free overfall. A professional camera (Contax 167MT) was used to film the brightened flow fields. Figure 1 shows schematic diagram of the arrangement of setup for flow visualization tests.

On the other hand, the mean velocity profiles upstream of a drop, across the falling and sliding jets, and inside the pool of a free overfall were all measured by an one-component FLDV (TSI 9832), operated in the back-scattering mode. The light source was a 4 W laser tube (Lexel 90-4). Only the green beam was used in this study. The positioning of the measuring volume of FLDV could be accurately controlled by three optical meters and three digital monitors (with precision higher than 0.01 mm). Note that the diameter of the measuring volume of FLDV was either 0.04 or 0.08 mm, depending upon the focal lenses used (TSI 9253-120 or 9118-250).

The definition sketch of flow field and of coordinate system used in this study is presented in Fig.2; in which X and y are the streamwise and vertical coordinates, respectively, with the origin at the toe of the drop structure. Moreover, Q is the discharge per unit width; U_o and Y_o are the depth-averaged velocity and flow depth of the approaching flow, respectively; U_c is the depth-averaged critical velocity and Y_c is the critical depth; H denotes the height of a drop; L_p and Y_p are the length and depth of the pool, respectively; and Y_1 is the flow depth at the base of a drop structure. In this work, the Froude number of the approaching flow is defined as $Fr = u_0 / \sqrt{gY_0}$.

EXPERIMENTAL RESULTS

Photo 1(a) shows flow visualization results concerning the instantaneous flow patterns in the sliding jets and inside the pools of three free overfalls for the relative critical depth Y_c/H (or Fr) = 0.146 (0.87). We can obviously find that a large-scale circulating flow exists in the pool with strong reverse flow near the base of the drop structure and with intense positive flow near the free surface of the pool. It seems that the greater the relative critical depth (or the Froude Number) the larger the size of the circulating vortex flow, i.e. the influence area of the circulating vortex flow inside the pool increases with the increasing Y_c/H (or Fr). It is also interesting to note that a shear layer exists between the sliding jet and the pool of a free overfall, where the velocity distribution varies sharply. As a supporting evidence, Photo 1(b) shows the magnified view of the interface between the sliding jet and the pool for Y_c/H (or Fr) = 0.146 (0.87), revealing the existence of a shear layer. By observing the flow fields underlying these photos, flow characteristics of the shear layer and the pool could be further evidenced. However, the detailed structure of the shear layer between the sliding jet and the pool, such as velocity distribution could be elucidated by using FLDV.

Figure 3 shows the measurement results made in a typical experiment for Y_c/H = 0.353, including not only the water surface profiles upstream of the drop structure as well as of the falling and sliding jets; but also some velocity profiles of and close to the sliding jet. The velocity distribution across the sliding jet, as seen in the measuring sections from 1 to 5 of Fig. 3, is basically uniform until the jet has touched the boundary of the pool. Note that the velocity profiles across the sliding jet and its vicinity, as evidenced in the measuring sections 1 and 2 in Fig. 3, are very similar to those in a turbulent jet, indicating again the existence of a shear layer with strong mixing between the sliding jet and the pool.

Utilizing these jet-like velocity profiles, the discharge of the circulating flow inside the pool, Q_c, could be accurately calculated if the positioning (or traversing) system is quite precise, the measuring technique is of non-intrusive type (e.g. FLDV), and the dimensions of the sensing probe are very small. All of these three conditions were fully satisfied in the present investigation, in which the positioning error was smaller than 0.01 mm and the diameter of the measuring volume of the non-intrusive FLDV is only either 0.04 or 0.08 mm depending upon the focal lens used. The variation of the realtive circulating dischsrge Q_c/Q with Y_c/H of this study is illustrated in Fig. 4. in which the corresponding results obtained by Rajaratnam and Chamani (1995) (using Prandtl probe of external diameter of either 3.2 or 2.6 mm) are also included. Focusing on the results of the present investigation, Q_c/Q decreases from about 0.6 for Y_c/H = 0.075 to about 0.17 for Y_c/H = 0.48 and the regression curve is well described by the equation (correlation coefficient is 0.993) :

$$\frac{Q_c}{Q} = 0.1079 \left(\frac{Y_c}{H}\right)^{-0.6163} \quad (1)$$

From Fig. 4, it can be also seen that, although overall trends of the present study and that of Rajaratnam and Chamani are somewhat similar (i.e. Q_c/Q decreases with increasing Y_c/H), the results of the latter are greater and smaller, respectively, than those of this study for Y_c/H < 0.125 and for Y_c/H > 0.125. It is suspected that the significant difference might arise from both interference effect induced by the intrusion of the sensing probe into the flow and from, more importantly, considerable size (thus with insufficient spacial resolution) of the sensor used in Rajaranam and Chamani (1995).

Figure 5(a) shows the profiles of the horizontal mean velocity $\overline{u}$ measured at ten verticals inside the pool of a free overfall for Y_c/H = 0.353 (Fr = 1.32) and X ranging from 8.5 to 80.0 mm. As seen in Fig. 5 for X = 8.5 ~ 80.0 mm, the value of u decreases rapidly from zero at the bottom to a local negative maximum at some y position, then increases gradually up to zero at about y = 20 - 25 mm, and finally becomes positive and increases with increasing y until the (mean) free surface has been reached. Note that a tiny part of the mean velocity profile close to the base of the drop, measured at X = 8.5 mm, shows existence of positive flow, partially reflecting the entrainment effect of circulating stream on the corner flow. Globally speaking, it is seen that a large-scale circulating flow actually exists in the pool with strong reverse flow near the base of the drop structure and with intense positive flow near the free surface of the pool, confirming both quantitatively and qualitatively the flow characteristics as illustrated in Photo 1(a).

Similarly, the profiles of the horizontal mean velocity $\overline{u}$ measured at different verticals inside the pool of a free overfall for Y_c/H=0.218 (F_r = 1.08) and 0.146 (0.87) are shown in Fig. 5 (b,c) respectively. Note that on each profile the solid curve connecting the data points is used for visual aid.

If we use the height of the pool as a characteristic length scale and adopt the maximum negative velocity u_m (occurring near the bottom) as a characteristic velocity scale, both measured at each vertical. Then the corresponding non-dimensional velocity profiles of Fig.5 (a-c) can be presented by Fig.6 (a-c). It is found that a similarity profile for the non-dimensionalized mean horizontal velocity does exist in the pool of a free overfall, not only for the case of supercritical approaching flow (F_r >1) but also for the case of subcritical oncoming flow (F_r <1). Regression analysis shows that the unique similarity profile can be expressed as

$$\frac{\overline{u}}{\overline{u}_m} = \begin{cases} -3.05 \left(\frac{y}{y_p}\right)^{\frac{1}{7}} \left\{1 - \mathrm{erf}\left[1.74 \left(\frac{y}{y_p}\right)\right]\right\} + 0.8, & \text{for } y > 0 \\ 0 & \text{, for } y = 0 \end{cases} \quad (2)$$

The above equation is valid for $0.3 \le X/L_p < 0.58$.

CONCLUSION

The characteristics of the velocity fields of free overfalls, with upstream subcritical and supercritical approaching-flow conditions, have been elucidated both qualitatively and quantitatively in this work. Some innovative results of this study have been presented of the vortex structures and mean velocity profiles inside the pools. An unique similarity profile of the mean horizontal velocity measured inside the pool has been presented first both for supercritical and subcritical approaching flow conditions.

REFERENCES

Gill, M. A., 1979,"Hydraulics of rectangular vertical drop structures," *Journal of Hydraulic Research*, Vol. 17, No. 4, pp. 289-302.

Marchi, E., 1993,"On the free overfall," *Journal of Hydraulic Research*, Vol. 31, No. 6, pp. 777-790.

Moore, W.L., 1943,"Energy loss at the base of free overfall," *Transactions, ASCE*, Vol. 108, pp. 1343-1360.

Rajaratnam, N. and Chamani M. R., 1995,"Energy loss at drops," *Journal of Hydraulic Research*, Vol. 33, No. 3, pp. 373-384.

Rand, W., 1955,"Flow geometry at straight drop spillways," *Proceedings of the American Society of Civil Engineers*, Vol. 81, No. 791, pp. 1-13.

Rouse, H., 1936,"Discharge characteristics of the free overfall," *Civil Engineering*, Vol. 6, No. 4.

White, M. P., 1943,"Discussion of Moore," *Transactions, ASCE*, Vol. 108, pp. 1361-1364.

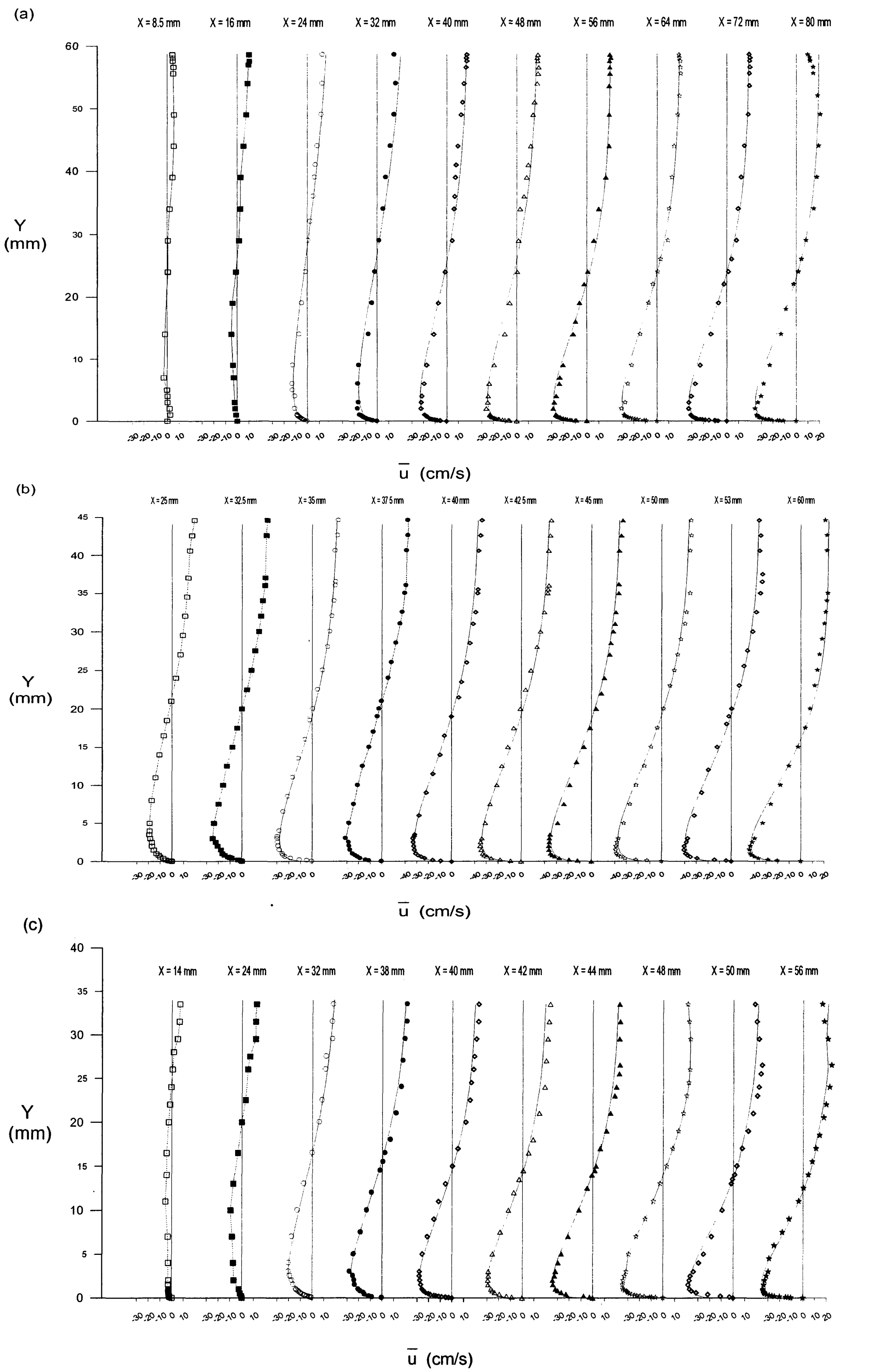

Fig.5 Vertical distributions of the mean horizontal velocity measured at different sections.
(a) $Y_c/H = 0.353$, (b) $Y_c/H = 0.218$, (c) $Y_c/H = 0.146$.

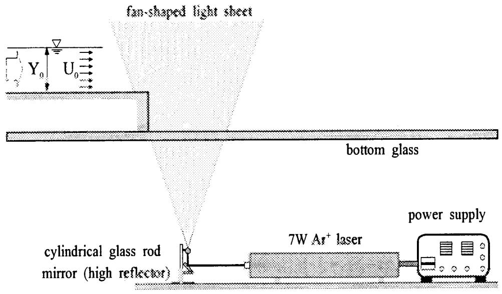

Fig. 1 Arrangement of setup for flow visualization tests.

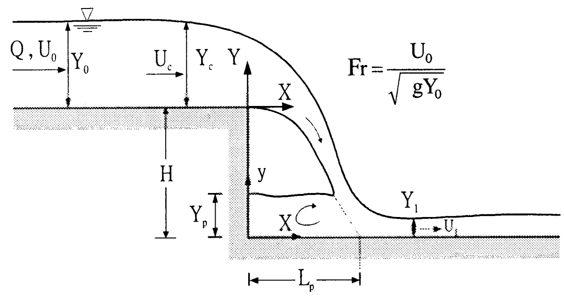

Fig. 2 Sketch of coordinate system and definition used.

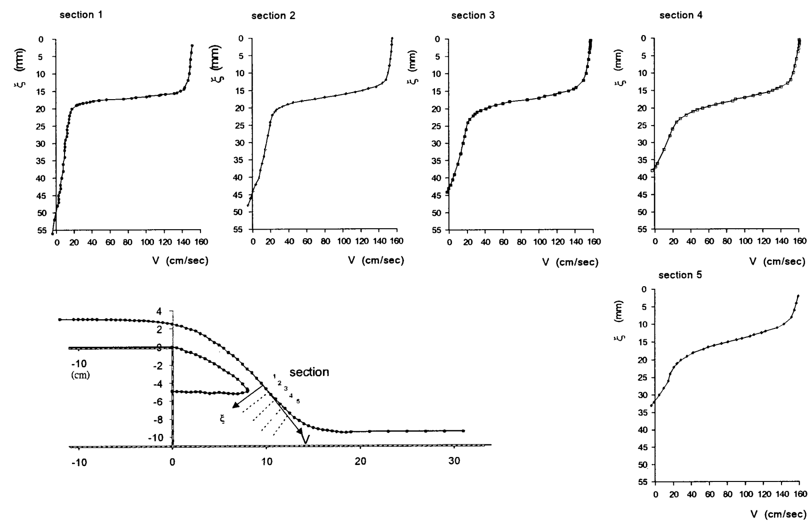

Fig. 3 Velocity profiles measured at different sections of the sliding jet of a free overfall for Yc / H = 0.353 (Fr = 1.32).

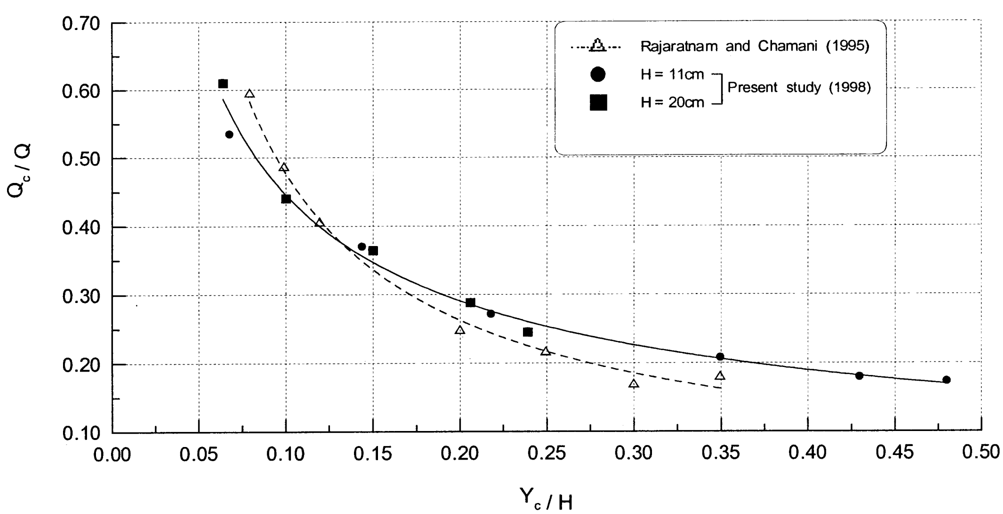

Fig. 4 Variation of Q_c/Q with Y_c/H.

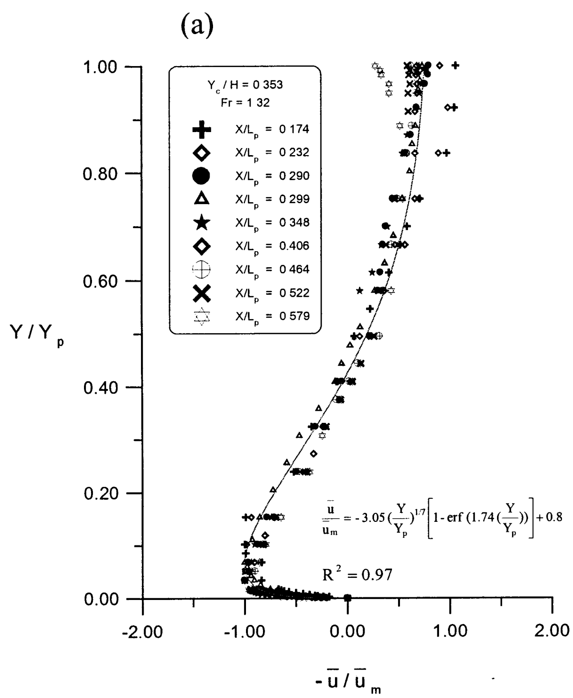

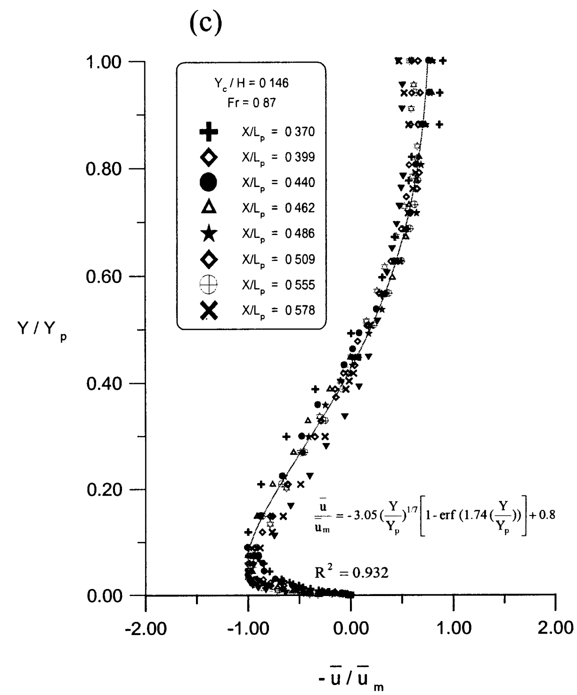

Fig.6 Non-dimensionalized profile of the mean horizontal velocity measured inside the pool of a free overfall. (a) $Y_c/H = 0.353$, (b) $Y_c/H = 0.218$, (c) $Y_c/H = 0.146$.

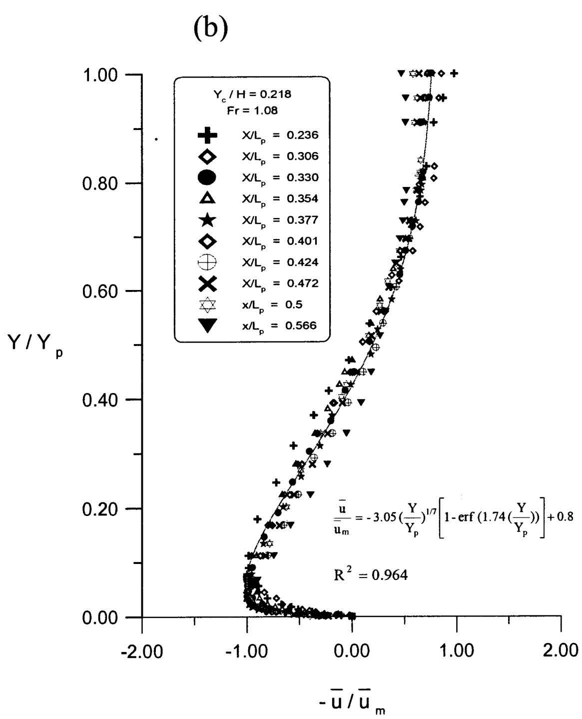

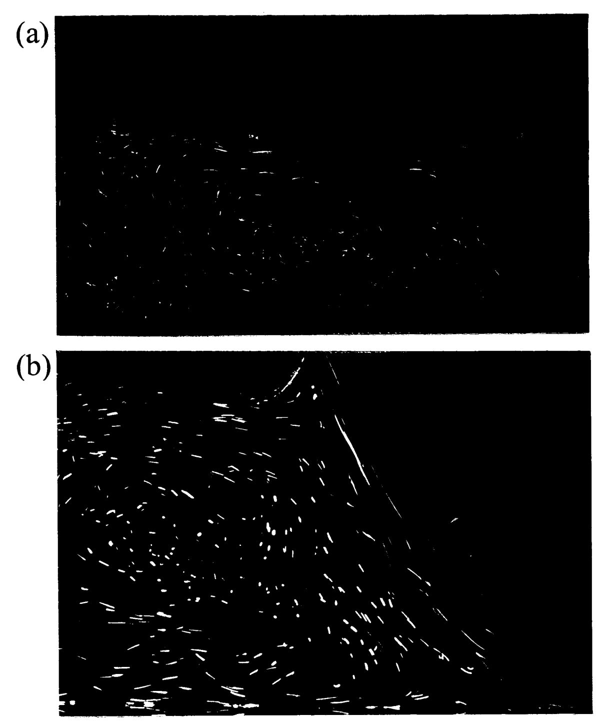

Photo 1 Instantaneous flow patterns for (a) Y_c/H (or Fr) = 0.146 (0.87); (b) magnified view of the same case as (a).